Available online at www.sciencedirect.com

SCIENCE DIRECT®

Tectonophysics 397 (2005) 93–111

TECTONOPHYSICS

www.elsevier.com/locate/tecto

Influence of the Neotethys rifting on the development of the Dampier Sub-basin (North West Shelf of Australia), highlighted by subsidence modelling

Laurent Langhi*, Gilles D. Borel[1]

Institute of Geology and Palaeontology, University of Lausanne, CH-1015 Lausanne, Switzerland

Received 1 October 2003; accepted 19 October 2004
Available online 28 December 2004

Abstract

During the Late Palaeozoic and the Mesozoic, the development and evolution of the North West Shelf of Australia have been mostly driven by rifting phases associated with the break-up of Gondwana. These extensional episodes, which culminated in the opening of the Neotethys Ocean during the Permo-Carboniferous and a series of abyssal plains during the Jurassic-Cretaceous, are characterised by different stress regimes and modes of extension, and therefore had distinctive effects on the margin, and particularly on the Northern Carnarvon Basin.

Interpretation of 3D and 2D seismic data enables a structural and stratigraphic analysis of the Late Palaeozoic sediments deposited in the proximal part of the Dampier Sub-basin (Mermaid Nose). Based on their seismic characters, stratigraphic relationship, internal patterns, lateral continuity, and architecture, these units are associated here with the Pennsylvanian?–Early Sakmarian glaciogenic Lyons Group and the Sakmarian–Artinskian Callytharra Formation. The former were deposited in a half-graben whose development is associated with the onset of the Neotethys rifting, and the latter is characterised by restricted deposition, inversion of prograding patterns, and uplift.

The integration of seismo-stratigraphic characterisation of the Late Palaeozoic sequences and Mesozoic data from one exploration well (Roebuck-1) enables the construction of subsidence curves for the Mermaid Nose and the interpretation of its geohistory.

The tectonic subsidence curves show a striking Permo-Carboniferous rifting phase related to the Neotethys rifting and a discrete Late Jurassic–Early Cretaceous event coeval with the opening and the spreading of the Argo Abyssal Plain.

This result points out the predominance of the effects of the Permo-Carboniferous Neotethys episode, whereas the extension related to the Argo Abyssal Plain rifting that occurred later and closer to the studied area, had only limited effects on the

* Corresponding author. Tel.: +41 21 692 43 58; fax: +41 21 692 43 05.
E-mail address: Laurent.Langhi@unil.ch (L. Langhi).
[1] Present address: Geological State Museum, Lausanne, BFSH2 UNIL, CH-1015 Lausanne, Switzerland.

0040-1951/$ - see front matter
doi:10.1016/j.tecto.2004.10.005

subsidence of the proximal Dampier Sub-basin. Therefore, it supports a tectonic model with two distinct modes of extension for the Late Palaeozoic (widespread) and the Mesozoic (localised) rifting phases.

Keywords: Seismic stratigraphy; Subsidence; Rifting; Glacial deposits; Neotethys; Western Australia

1. Introduction

The northwestern margin of Australia has been a long-term passive margin (Stagg and Colwell, 1994) that underwent a polyphase tectonic history associated with the break-up of Eastern Gondwana (Veevers, 2000; Borel and Stampfli, 2002). Several Phanerozoic sedimentary basins developed in association with different tectonic events culminating in the Late Palaeozoic opening of the Neotethys Ocean and a series of Mesozoic abyssal plains.

Both of these extensional episodes displayed different stress regimes (Fullerton et al., 1989; Hill, 1994) and modes of extension (Gartrell, 2000), and had distinctive effects on the margin and particularly on the Northern Carnarvon Basin.

On the northeastern Gondwana margin, the Permo-Carboniferous is marked by the initiation of the

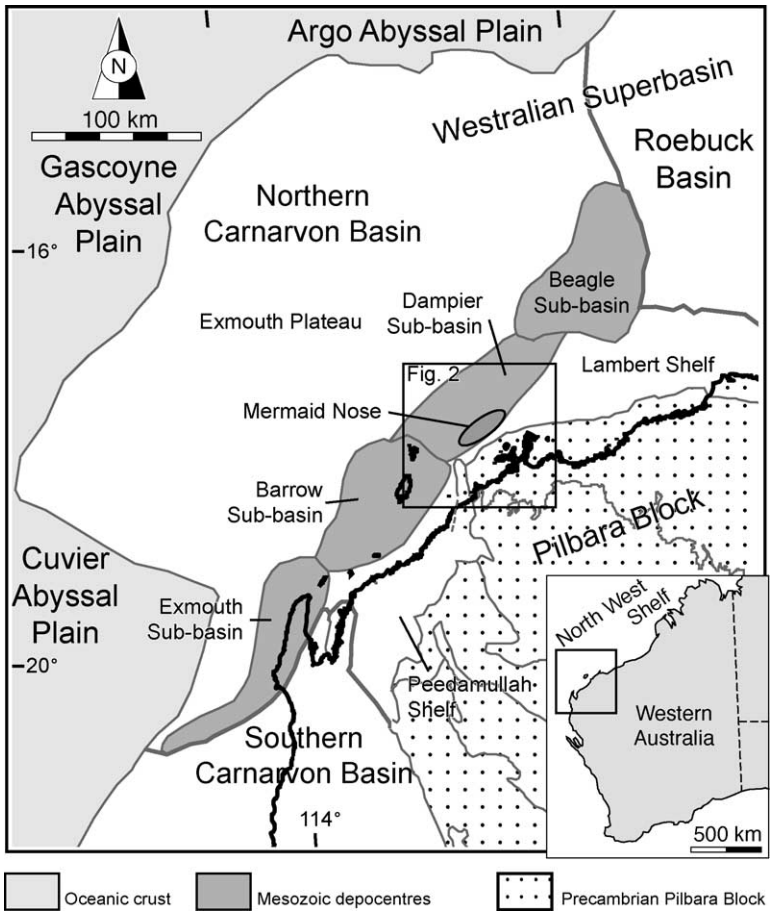

Fig. 1. Geological setting of the southern North West Shelf and the Northern Carnarvon Basin.

Neotethys rift system that propagated from Australia to the eastern Mediterranean area, removing slivers of the Gondwana continent (Stampfli, 2000; Stampfli et al., 2001a; Stampfli and Borel, 2002; Borel and Stampfli, 2002). On the northwestern margin of Australia, this rifting generated extensive deformation trending north–northeast (Gartrell, 2000) that defined the large-scale geometry of the margin and that formed the so-called Westralian Superbasin (Fig. 1, Yeates et al., 1987). These structures were subsequently overprinted by Mesozoic features coeval with the rifting of the abyssal plains (Figs. 1 and 2). This extension reactivated Permian features (Pryer et al., 2002) and developed new faults that formed restricted depocentres (Figs. 1 and 2) (Gartrell, 2000) with thick sections of Jurassic and Cretaceous deposits (Jablonski, 1997).

The purpose of this paper is, using seismic and well data, to have a thorough examination of the evolution of the proximal part of the Dampier Sub-basin (Northern Carnarvon Basin) during the two main successive extensional events affecting the northwestern margin of Australia. The integration of structural and stratigraphic analysis with subsidence modelling gives new constraints to understanding the development and the impact of the Late Palaeozoic and Mesozoic rift systems, and the response of the margin to these major events. In light of these new results, we support a model for the evolution of the proximal Dampier Sub-basin (i.e., Mermaid Nose, Figs. 1 and 2) that emphasizes the predominance of the effects of the Neotethys-related extensional episode versus the effects of the abyssal plains rifting.

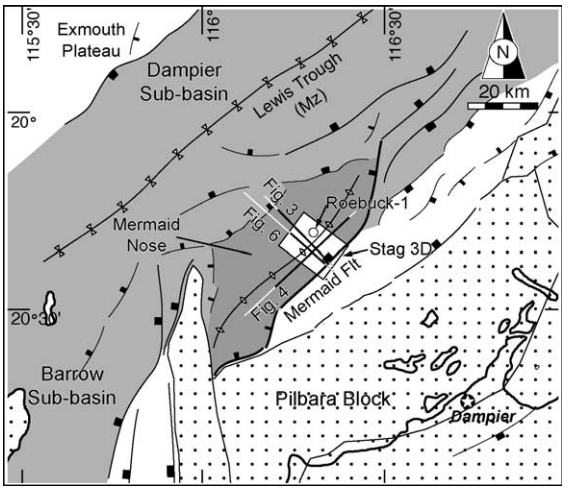

Fig. 2. Geological setting and structural elements of the Mermaid Nose area and the proximal Dampier Sub-basin. Location of well data, 3D seismic data and seismic sections shown in (Figs. 3, 4 and 6).

2. Geological setting

The northwestern Australian margin is made up of four Phanerozoic sedimentary basins that form the North West Shelf (Fig. 1, AGSO, 1994; Hocking et al., 1994). The northeast-trending Northern Carnarvon Basin (Fig. 1) is located at the southern end of the North West Shelf. It lies between the Argo and Gascoyne Abyssal Plains to the northwest, and the Precambrian Pilbara Block to the southeast (Fig. 1), and contains a maximum of 15 km of Palaeozoic to recent sedimentary infill (Hocking et al., 1987).

The Permo-Carboniferous rifting phase resulted in the definition of the dominant northeast-trending fabric (Fig. 1), with the development of the normal faults defining the boundary between the sedimentary basin and the Precambrian Pilbara Block (Figs. 1 and 2). This tectonic episode also resulted in the development of the large marginal Exmouth Plateau and shallower areas to the southeast, such as the Peedamullah Shelf or the Lambert Shelf (Fig. 1, see also Hocking et al., 1994). The present-day Mermaid Nose (studied area, Fig. 2), represents the southeasternmost part of the transition area between the deep plateau and the Pilbara Block (Figs. 1 and 2). Its initial development is associated with the Permo-Carboniferous rifting and the development of a large half-graben (Fig. 3).

The Mesozoic extensional episode is characterised by the development of a series of northeast-trending depocentres, such as the Dampier Sub-basin, lying between the large marginal plateau and the Precambrian basement (see Figs. 1 and 2). The Lewis Trough (Fig. 2) forms the main depocentre of the Dampier Sub-basin: it developed mainly during the Mesozoic extension and hosted up to several kilometres of Jurassic sediments overlain by a thick Cretaceous and Tertiary section. To the southeast

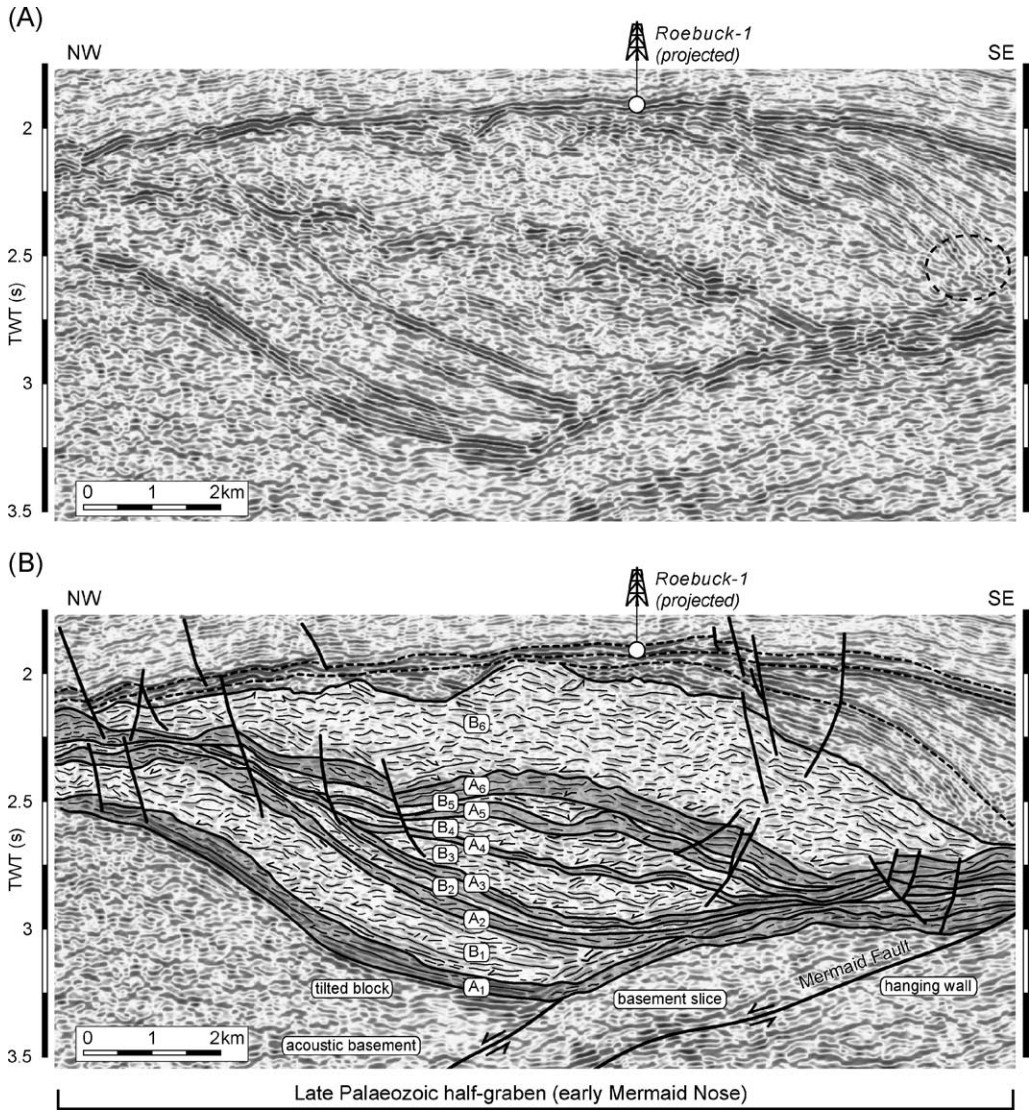

Fig. 3. Late Palaeozoic half-graben and configuration of the Lyons Group seismic facies. Location is shown on Fig. 2. (A) Uninterpreted seismic section (the circle—dotted line—shows an artefact due to the nearby presence of the Mermaid Fault plane). (B) Interpreted seismic section showing the glacial Permo-Carboniferous sequences architecture. The reflective facies (labelled An) form thin veneer of basal deposit overlain by thick low/moderate amplitude reflectors (labelled Bn) interpreted as paraglacial succession.

(Fig. 2), the proximal part of the sub-basin (including the Mermaid Nose) marks the transition to the shelf area and the Pilbara Block (Fig. 2), and is also affected by this Mesozoic extension. From the Triassic to the Early Cretaceous, the Mermaid Fault was reactivated, leading to the development of a rollover anticline that finalised the structure of the Mermaid Nose (Fig. 2).

3. Data

The seismic dataset used for the stratigraphic and structural analysis is located over the Mermaid Nose (Fig. 2). It includes a 110 km^2 seismic volume going down to 3.5 s TWT (H93S Stag 3D M.S.S. or Stag 3D on Fig. 2), in parallel with regional northwest- or southeast-trending seismic lines reaching to 6 s TWT

(Fig. 2). Due to the data processing that was focussed on shallower Jurassic–Cretaceous targets (ca. 0.75 s TWT), the final migrated seismic data displays a pre-Triassic section of poor quality. Therefore, attributes related to reflection strength and phase were the keys to tracking the main discontinuities, and strengthened the distinction between sedimentary cover and basement rocks and between sedimentary sequences.

In order to define the thickness of the sedimentary sequences, a velocity law has been calculated on the basis of the integration of the available regional time–depth curves, and has been extrapolated down to the Permo-Carboniferous section.

Several wells have been drilled on the Mermaid Nose, with most of them reaching the Early Cretaceous to Late Jurassic sequences. Roebuck-1 (Fig. 2) was drilled in 2000, and is the deepest well of the area, reaching the Permian Chinty Formation at 2871 mRT (meter below the rotary table). It therefore provides the best stratigraphic control for construction of the subsidence curves.

4. Late Palaeozoic seismic stratigraphy

Despite the poor stratigraphic control from well data, depositional environments were inferred for the Late Palaeozoic units. Seismic facies analysis, based upon seismic character, stratigraphic relationships, internal patterns, and architecture, enabled the identification of a series of seismo-stratigraphic units within the Late Carboniferous to Early Permian section.

4.1. Permo-Carboniferous units

During the Permo-Carboniferous, periods of glaciation affected much of high-latitude Gondwana, as highlighted by the widespread glaciogenic sediments that were deposited in South America, South Africa, Antarctica, on the Arabian Peninsula, and in India, Pakistan, and Australia (Levell et al., 1988; Alsharhan, 1993; Eyles and Young, 1994; Potter et al., 1995; Mishra, 1996; Archbold, 2002; Redfern and Williams, 2002.

In the Northern Carnarvon Basin, the oldest Westralian Superbasin sequence is composed of Permo-Carboniferous sediments (AGSO, 1994; Stagg and Colwell, 1994) of the glaciogenic Lyons Group (Hocking, 1990). This sequence has also been recognised on the Peedamullah Shelf, located approximately 100 km southwest of the studied area (Fig. 1), where it unconformably overlies the Early Carboniferous Quail Formation (Iasky et al., 2002; Yasin and Iasky, 1998). Therefore, despite the lack of stratigraphic control, the Early Permian (and Carboniferous?) sequences present on the Mermaid Nose are also correlated with the Lyons Group.

4.1.1. Seismic facies, Permo-Carboniferous

On the Mermaid Nose, the interpreted Late Palaeozoic units are mainly preserved within a half graben (100×40 km, Fig. 2) defined by the rotation of a basement block along the Mermaid Fault (Fig. 3). The seismo-stratigraphic interpretation, based on reflection amplitude and frequency, internal patterns, and architecture, allows the subdivision of the Permo-Carboniferous package into 6 stacked seismo-stratigraphic units, simply called “units” hereafter (i.e., A1–B1 to A6–B6, Fig. 3), that successively filled in the depocentre. These units probably lie directly above the basement rock as shown in Fig. 3. Each of them is composed of two main successive seismic facies with a highly reflective facies (A, Fig. 3), which truncate the underlying units and veneer the topography, and each unit is followed by a usually thicker (up to 1000 m) transparent facies (B, Fig. 3) filling in the negative relief.

The A-type facies, characterised by high amplitude and high frequency reflections, is widespread in the incipient depocentres (Fig. 3). The lower boundary usually represents a surface of truncations with well-developed angular unconformities. This seismic facies is typically composed of a few continuous to subcontinuous reflectors that follow and drape the underlying deposits (Fig. 3), extending over both sides of the depocentre and forming veneers of deposits. The upper bounding surface usually corresponds to an onlap surface.

Seismic facies B (Fig. 3) is characterised by subcontinuous to discontinuous and low/moderate amplitude reflections. It often fills in restricted structures and depocentres left by underlying units and displays shingled progradation, basin fill, and complex fill reflection patterns as defined by Mitchum et al. (1977). The upper boundary typically displays

an erosional limit with well-marked angular unconformities (Fig. 3).

Fig. 4 shows a more detailed interpreted section of the younger unit (A6–B6 on Fig. 3). It reveals a basal sequence (A6, Fig. 4) overlain by six stratigraphic sequences (B61 to B66, Fig. 4), forming the last B-type seismic facies (B6, Fig. 4).

4.1.2. Geologic interpretation, Permo-Carboniferous

The first deposits present on the Mermaid Nose display two types of seismic facies easily distinguishable from the chaotic basement. The repetition of the successive units (A1–B1 to A6–B6 on Fig. 3) suggests the influence of an event of cyclic character.

The six successive reflective A-type seismic facies display roughly similar distribution and characteristics. They constantly truncate the underlying unit and draped the newly formed relief, extending laterally over both flanks of the depocentres (Figs. 3 and 4). The strong amplitude contrast between seismic facies A and the layers directly below and above (Fig. 3) suggests significantly compacted and consolidated sediment for seismic facies A (Pfiffner et al., 1997). Boulton (1978) and Boulton and Deynoux (1981) suggest that only basal accumulations beneath a shearing glacier have this characteristic. Based on such features, and emphasized by the facies distribution and stratigraphic position, these deposits (seismic facies A) are interpreted as possible basal moraines deposited at the interface between the bedrock and a moving ice mass (glacier retreat and advance, Fig. 5A). Mapping of the younger and best-preserved of these inferred basal moraines (A6, Fig. 4) reveals a paleosurface with a maximum relief of around 400 m.

The low- to moderate-amplitude B-type seismic facies fill in the underlying structures and depocentres and onlap the basal moraine. They form elongate lenticular bodies that can be restricted close to the axis of the depocentre, or can stretch over the entire Mermaid Nose and thin out towards the margin of the depocentre (Fig. 3). Due to the absence of stratigraphic control from well data, no sedimentologic interpretation can be unambiguously inferred; nevertheless, based on seismic facies distribution and architecture, the B-type facies are interpreted as paraglacial deposits. This general term refers to glacier-related sediments, and only denotes a spatial proximity to the ice mass. On the Mermaid Nose, such sediments were possibly deposited in front of the ice mass, and derived from the partial melting and retreat of the glacier. This scenario is supported by the detailed interpretation of the youngest and best-

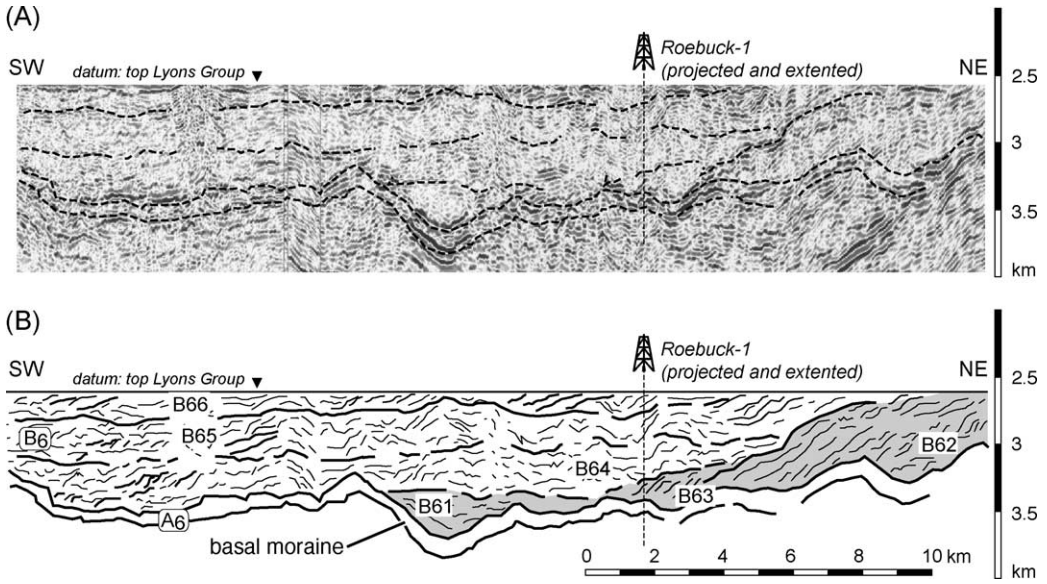

Fig. 4. Flattened depth-converted cross section showing the youngest Permo-Carboniferous Lyons Group stacked unit (A6–B6). Location is shown on Fig. 2. (A) Uninterpreted seismic section. (B) Interpreted seismic section showing the inferred ice-marginal fans (B61–B63, in grey) followed by prograding deposits filling in the remaining Late Palaeozoic depocentres (B64–B66).

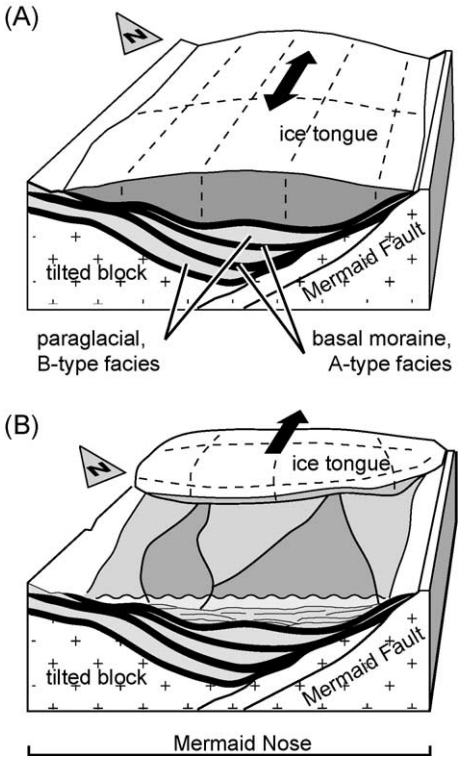

Fig. 5. Conceptual model for the glaciogenic sediments deposition on the Mermaid Nose. (A) Glacier advance phase and deposition of the thin and reflective seismic facies (A-type facies) interpreted as a basal moraine. (B) Glacier retreat phase and deposition of paraglacial sediments (B-type facies) in glaciofluvial to glaciomarine environment.

preserved B-type facies on Fig. 4. It presents a succession of six subaqueous sequences interpreted as restricted ice marginal fans (B61, B62 and B63 on Fig. 4), followed by the complete flooding of the half-graben and the deposition of thick sequences (B64, B65 and B66 on Fig. 4) filling in the depocentres.

Furthermore, the transparent B-type facies present strong analogies with some meltout or reworked till observed in the glacial series of the Rhône Valley in the Swiss Alps (Pfiffner et al., 1997). These packages could be correlated with poorly sorted sediments (Eyles et al., 1990) deposited during a phase of retreat and melting of the glacier, and subsequently truncated during the following phase of glacier advance (Fig. 5).

Despite poor constraints on the age of the glaciogenic deposits, it is commonplace to assign a Pennsylvanian to Early Sakmarian age for the last glacial event affecting the western Australian margin (e.g. Hocking, 1990; Dickins, 1996; Wopfner, 1999; Archbold, 2002; Eyles et al., 2003). On the North West Shelf, the Grant Group in the Canning Basin and the Lyons Group in the Northern Carnarvon Basin are commonly assigned to this Permo-Carboniferous glacial episode (Hocking, 1990; Redfern and Williams, 2002). Pennsylvanian? to Early Sakmarian glacially influenced marine strata of the Lyons Group have been drilled and investigated on the Peedamullah Shelf, adjacent to the Mermaid Nose (e.g. Iasky et al., 2002; Eyles et al., 2003), where they range from sandstone to siltstone (Eyles et al., 2003). The successive glacial facies interpreted on the Mermaid Nose (A1–B1 to A6–B6) are therefore proposed as an equivalent of the Lyons Group.

4.2. Early Permian sequences

In the Northern Carnarvon Basin, occurrences of sediments deposited in a shallow marine environment, under warmer conditions (Callytharra Formation), have been reported during the Sakmarian (Iasky et al., 2002). On the Peedamullah Shelf (Fig. 1), as well as in the Southern Carnarvon Basin (Baker et al., 2000), these sediments overlaid the Lyons Group and were deposited until the Artinskian (Mory and Backhouse, 1997).

4.2.1. Seismic facies, Early Permian

On the Mermaid Nose, a restricted sedimentary package partially overlies the glacial sequences and forms a sedimentary wedge (Fig. 6). Southeastward stratigraphic thickening of this package (Fig. 6) implies a reactivation (normal displacement) of the Mermaid Fault. This seismic unit displays an overall facies that considerably differs from the underlying glaciogenic sequences, and is divisible into 3 seismic facies (from bottom to top: C, D and E on Fig. 6).

Seismic facies C (Fig. 6) is composed of relatively continuous reflectors of high amplitude. Its lower boundary is characterised by onlap terminations and onlap infill of depressions inherited from the underlying glaciogenic sequence (sequence B6 on Fig. 6). The internal configuration is characterised by parallel reflections with packages in thin prograding patterns. The upper boundary of sequence C displays, to the southeast, a concordant contact with the overlying

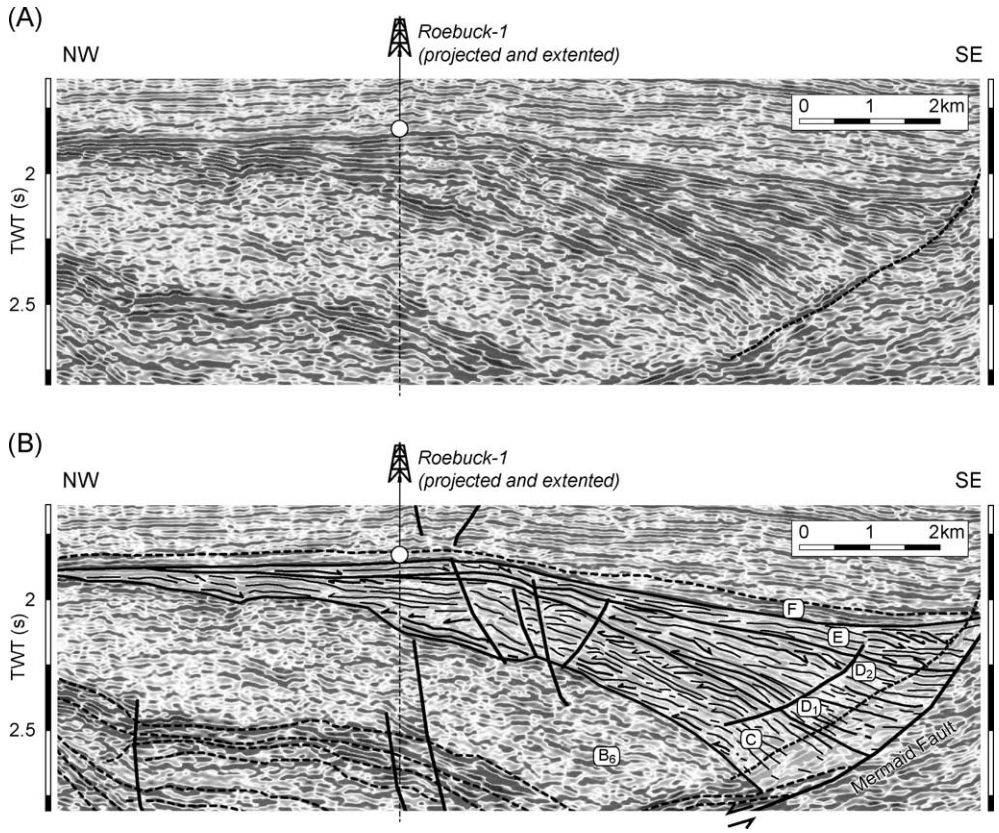

Fig. 6. Post glacial Permian units on the Mermaid Nose. Location is shown on Fig. 2. (A) Uninterpreted seismic section (the vicinity of the Mermaid Fault plane shows an artefact—dotted line—due to the nearby presence of the Mermaid Fault plane). (B) Interpreted seismic section showing the seismic facies architecture within the sedimentary wedge equivalent to the Callytharra Formation (Sakmarian–Artinskian) and the overlying Late Permian Chinty Formation.

sequence (sequence D on Fig. 6), which turns, to the northwest, into an angular unconformity that suggests a truncation (Fig. 6).

Seismic facies D (Fig. 6) has a wedge geometry and is composed of semi-continuous reflectors with moderate/high amplitude. The base of this sequence (D1 on Fig. 6) is characterised by onlap terminations and northwestward-shingled prograding patterns (Fig. 6), which turn into southeastward-prograding patterns near the top of the sequence (D2 on Fig. 6). A few reflections displaying divergent patterns occur near the Mermaid Fault (Fig. 6).

High amplitude and continuous reflectors form seismic facies E (Fig. 6). The sequence is characterised by southeastward-prograding clinoforms with toplap terminations forming its upper boundary (Fig. 6). These deposits completely filled in the remains of the Late Carboniferous–Early Permian depocentres (Fig. 6).

4.2.2. Geologic interpretation, Early Permian

Based on their vertical position and on their acoustic character with moderate/high amplitude and good continuity, and their internal configuration, facies C, D, and E have been correlated with the marine Sakmarian–Artinskian Callytharra Formation present on the Peedamullah Shelf (Iasky et al., 2002) (Fig. 1).

Sequence C (Fig. 7A) overlies the last paraglacial sequence (B6, Figs. 3, 6 and 7), and represents a new flooding episode on the Mermaid Nose. The lower boundary, characterised by an onlap surface and the presence of onlap fill patterns, suggests that

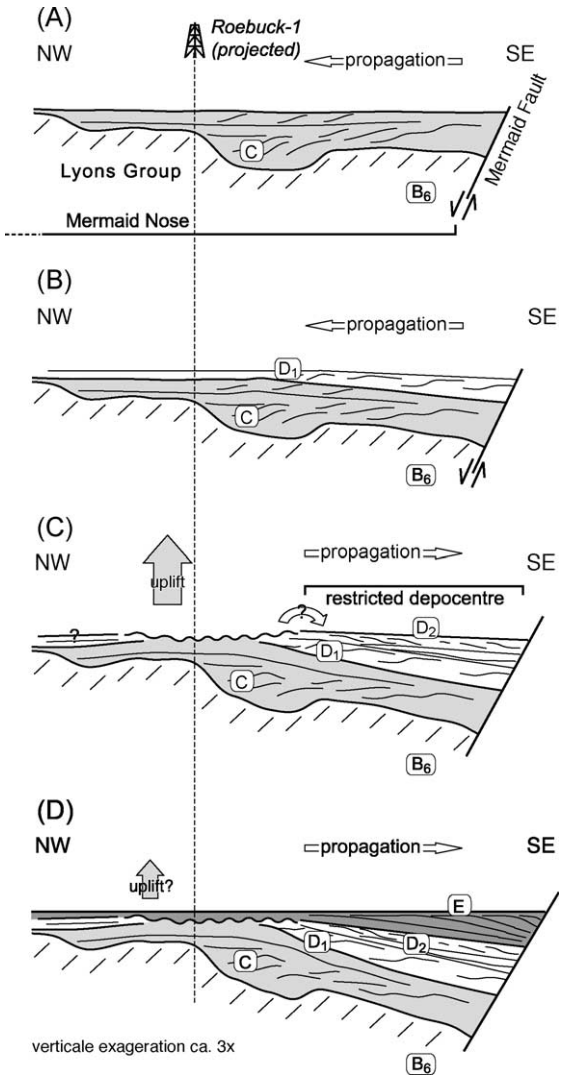

Fig. 7. Schematic evolution of the Sakmarian–Artinskian sedimentary wedge on the Mermaid Nose. (A) North–westward prograding sequence C deposited over a paleorelief left by the Lyons Group. (B) North–westward deposition of the lower part of the sequence D (D1). (C) Possible syn-tectonic deposits overlain by south–eastward prograding sediments of uppermost sequence D (D2) coeval with uplift and erosion. (D) Final south–eastward prograding clinoforms with toplap terminations (E) coeval with possible uplift and local erosion.

these sediments were deposited over a paleorelief inherited from the previous episode (i.e., unit B6, Figs. 6 and 7). In the upper part of sequence C, a northwestward progradation is suggested by thin, shingled clinoforms.

The lower part of sequence D (D1 on Figs. 6 and 7) is characterised by a shingled configuration, prograding occasionally to the northwest (Fig. 7B). The top of the sequence (D2 on Figs. 6 and 7) displays south-eastward-prograding foresets, and was deposited in a restricted depocentre adjacent to the Mermaid Fault (Fig. 7C), while uplift and erosion possibly started in the northwestern part of the Mermaid Nose and truncated the underlying sequence (D1 and C, Fig. 7C). A similar southeastward direction of progradation is also observed within sequence E (Fig. 7C and D), which is also more developed to the southeast part of the Mermaid Nose (Fig. 7D).

This change in sediment distribution (from northwestward progradation in sequences C and D1 to southeastward progradation in sequences D2 and E, Fig. 7) suggests a local but important change in the Early Permian deposition process. This change results from a probable uplift of the Mermaid Nose during the late deposition of the Callytharra equivalent (Late Sakmarian to Early Artinskian, Fig. 7C and D).

5. Other Permian units, Mermaid Nose

In the Northern Carnarvon Basin and the distal Dampier Sub-basin, the late Early Permian (Artinskian–Kungurian) is generally associated with the Wooramel and Byro Groups (Mory and Backhouse, 1997; Baker et al., 2000). On the Peedamullah Shelf, lying in a similar position to the Mermaid Nose (Fig. 1), such late Early Permian marine, shoreface, and deltaic formations are absent, and the Sakmarian–Artinskian Callytharra Formation is directly overlain by Late Permian deposits of the Kennedy Group (Iasky et al., 2002; Eyles et al., 2003). On the Mermaid Nose, the Late Carboniferous–Early Permian glaciogenic units and the marine wedge are overlain by a thin sequence (sequence F on Fig. 6) with sub-parallel and discontinuous to semi-continuous reflectors.

On the basis of the interpretation of Roebuck-1 (Fig. 8), this sequence is interpreted as the Chinty Formation, a distinct unit within the Kennedy Group (Mory and Backhouse, 1997; Gorter and Davies, 1999). The geometry of the reflectors suggests deposition over a stable surface, without major

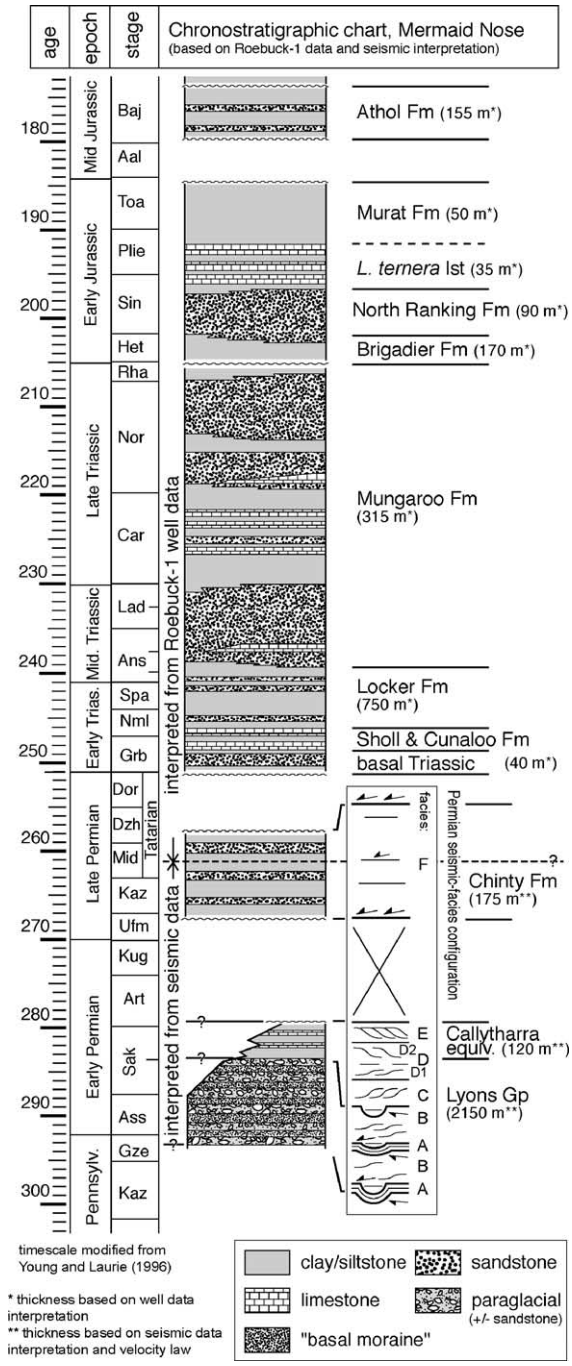

Fig. 8. Chronostratigraphic chart for the Mermaid Nose.

tectonic events. It represents a renewal of sedimentation after an episode of erosion/non-deposition during the late Early Permian (Fig. 8).

6. Mesozoic stratigraphy

Numerous detailed descriptions of Mesozoic and Cainozoic stratigraphy for the Dampier Sub-basin have been published. For general Mesozoic stratigraphy, the reader is referred to Boote and Kirk (1989), Labutis (1994), Miller and Smith (1996), Westphal and Aigner (1997), Romine et al. (1997), and Jablonski (1997). Gorter (1994), Barber (1994), and Young et al. (2001) provide detailed stratigraphy for the Triassic, Late Jurassic–Early Cretaceous, and middle Cretaceous-recent sequences, respectively.

The generalised chronostratigraphic column on the Mermaid Nose for the Mesozoic section, from the Triassic to the Middle Jurassic, is described in Fig. 8. It starts with the Locker Formation, which was deposited over a basal sandstone and two thin limestone sequences (Sholl and Cunaloo Formations on Fig. 8). The fluviodeltaic Mungaroo Formation (Gorter, 1994) was deposited during the Middle and Late Triassic, and was followed by the Brigadier and North Rankin Formations (Fig. 8). These Early Jurassic sandstones were overlain by carbonate and siltstone during the Pliensbachian and the Toarcian (*L. ternera* limestone and Murat Formation on Fig. 8). On the basis of the analysis of the Stag-1 data (located ca. 2 km south of Roebuck-1, Fig. 2), Crowley and Collins (1996) give a detailed description of the Cretaceous section for the studied area. The "Berriasian sandstone", which overlies the Bathonian–Bajocian Athol Formation, is followed by a series of sandstone and shale units, separated by several hiatuses up to the Campanian (lower Muderong Shale, M. australis Sandstone, upper Muderong Shale, and Gearl siltstone and Withnell Formation on Table 1).

7. Subsidence analysis

The Late Palaeozoic and Mesozoic evolution of the proximal part of the Dampier Sub-basin, in terms of tectonic setting, timing of the onset of rifting, and basin infill, is documented by subsidence analysis. We will focus on the part of the subsidence that is controlled by crustal processes (tectonic or thermo-tectonic subsidence).

Table 1
Original data used for the subsidence curve calculation

Name	Thickness (m)	Age Top (Ma)	Age Base (Ma)	Erosion (m)	Bathy Max (m)	Bathy Min (m)
Top		0	10	0	80	80
Whitnell	150	70	79		60	50
HIATUS		79	91		0	0
Gearle Silstone	100	91	106		50	30
HIATUS		106	113		0	0
Upper Muderong Shale	130	113	119		60	20
M. australiasis Sandstone	30	119	121		30	10
HIATUS		121	122		60	0
Lower Moulderong Shale	25	122	130		60	10
HIATUS		130	135		60	0
Beriasian Sandstone	25	135	137		60	20
HIATUS		137	148		0	0
Erosion		148	152	150	0	0
Eliassen Legendre Fm?	150	152	168		30	10
Athol Fm	45	168	174		30	10
Athol Fm	155	174	179		20	0
HIATUS		179	185		0	0
Murat Fm	50	185	193		50	20
L. ternera Lst	35	193	197		70	20
North Rankin Fm	90	197	202		50	0
Brigadier Fm	170	202	205		30	10
HIATUS		205	206		0	0
Mungaroo Fm	140	206	220		20	0
Mungaroo Fm	35	220	225		30	10
Mungaroo Fm	50	225	232		30	0
Mungaroo Fm	90	232	238		10	0
Locker Fm	750	238	246		50	20
Culnaloo+Sholl+basal Trias	40	246	251		80	20
HIATUS		251	225	20	20	0
Chinty Fm (F)	175	255	269		20	0
HIATUS		269	278	20	0	0
Callytharra equiv. (E)	20	278	280		50	30
Callytharra hiatus		280	281	140	0	0
Callytharra equiv. no depot (D)	40	281	283		0	0
Callytharra equiv. (C)	100	283	285		100	50
Lyons last paraglacial	840	285	288		150	50
Lyons basal moraine	60	288	289		50	20
Lyons other	1250	289	296		150	0

The definition of the 37 events characterising the starting model is based on the seismic data and well data interpretation.

7.1. Data

The construction of the subsidence curves for the Mermaid Nose is partially based on the interpretation of Roebuck-1 well data. This well is the deepest one drilled on the Mermaid Nose, and therefore provides the best control for the definition of the sedimentary sequences. The basic data available for Roebuck-1 consists of cutting descriptions performed on every 5 or 10 m section from 330 mRT (meter below rotary table) to 2871 mRT. This data was interpreted on the basis of lithological (situ ecris lithological, vaut mieux utiliser geological, et non geologic, etc.) changes, and 18 formations were differentiated, from the Late Permian Chinty Formation (Fig. 8) to the Campanian Withnell Formation (Table 1).

Investigation of the Phanerozoic subsidence of the Dampier Sub-basin also requires considering and integrating the older (Permo-Carboniferous) sequences present below the Roebuck-1 total depth (Fig. 8).

Therefore, a downward extension of Roebuck-1 (Fig. 8) has been constructed based on the different sequences interpreted on the seismic data (Figs. 3, 4 and 6). Thicknesses were determined on the basis of a regional, recalculated velocity law, and ages were determined on the basis of published data (e.g., Hocking, 1990; Dickins, 1996; Archbold, 2002; Eyles et al., 2003 for the Lyons Group and Iasky et al., 2002 for the Callytharra equivalent). This information is summarised in Fig. 8 and Table 1.

Based on the Roebuck-1 data and the downward extension, 37 "events" were used to calculate a subsidence curve for the Mermaid Nose (Table 1).

7.2. Subsidence curves

Table 1 shows the starting model for the construction of the subsidence curves. It represents the different formations and the associated parameters necessary for the calculation of the subsidence of the Mermaid Nose. The definitions of these parameters result from the interpretation of the well and seismic data.

The depositional bathymetry, which represents a key parameter in subsidence analysis, has been estimated on the basis of the sedimentary structures and stratigraphic relationship for the Permo-Carboniferous sequences, and also the lithologies for the Mesozoic sequences (where well data is available). Table 1 shows a maximum and minimum estimate of the bathymetry for each time interval (i.e., each sequence). The paleobathymetry can be difficult to estimate, therefore the use of these two values (end-members) will enable the calculation of two options for the tectonic subsidence curve (Fig. 9).

The characterisation of the hiatuses in terms of deposition plus erosion, non-deposition, or only erosion, and their quantification in time, were estimated mainly on the basis of the architecture of the sequences and their stratigraphic relationships as observed on the seismic data. They were eventually further constrained by correlation with adjacent areas.

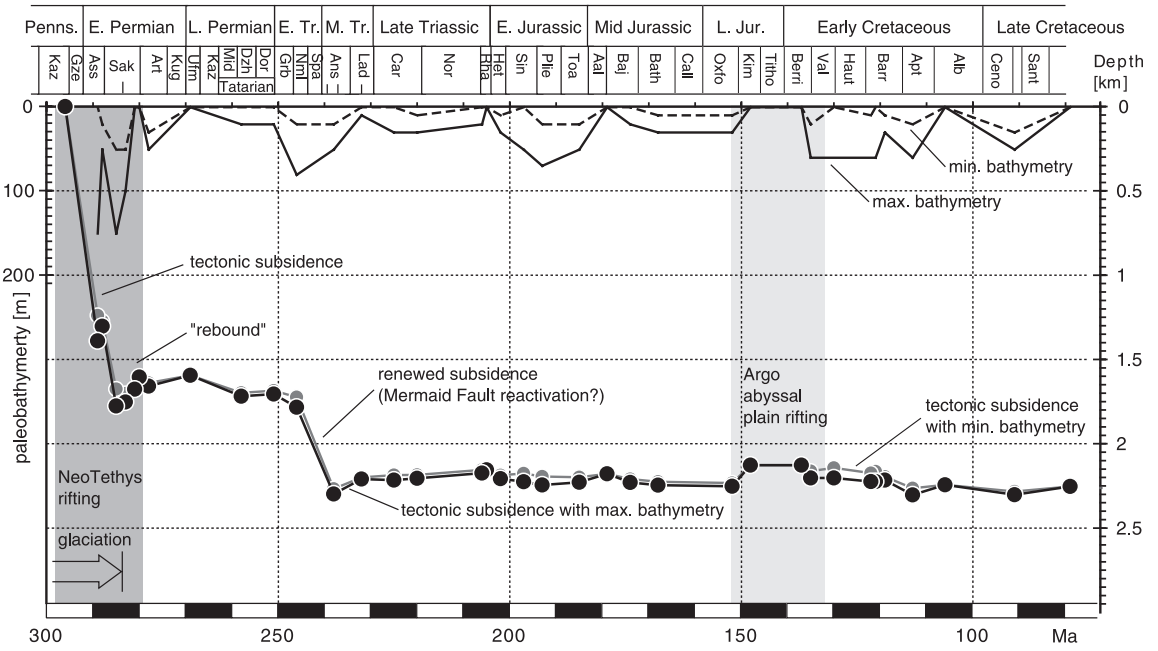

Fig. 9. Palaeozoic and Mesozoic geohistory of the Mermaid Nose. Interpreted tectonic subsidence curves with maximum and minimum bathymetry showing a geohistory punctuated by a major tectonic event during the Permo-Carboniferous and a discrete event during the Jurassic–Cretaceous, respectively, associated with the NeoTethys Ocean and the Argo Abyssal Plain opening processes. Well location is shown on Fig. 2 and starting model is shown on Table 1.

The result presented in Fig. 9, and discussed below, only shows the tectonic subsidence curves. These curves are built after removal of the effects of compaction and sediment and water loading (backstripping). The tectonic subsidence is calculated via the equation of Sclater and Christie (1980) or Bond and Kominz (1984), using a 1D model (Airy compensation) for sediment unloading. Therefore, the resulting curves reflect the tectonically driven part of the subsidence or the vertical evolution of the basement of the Mermaid Nose, driven only by the movements of the lithosphere. The qualitative interpretation of the subsidence will be discussed on the basis of the tectonic curve with maximum bathymetry correction (Table 1), which increases the shape of the curve and therefore allows a more straightforward interpretation.

As Sclater and Christie (1980) do not provide specific compaction parameters for glacial sediments, an alternative had to be found for the Lyons Group deposits. Based on the lithologies (sandstone to siltstone) reported from wells drilled on the Peedamullah Shelf (Eyles et al., 2003), and the proximal depositional setting interpreted from seismic data, the Permo-Carboniferous Lyons sediments of the Mermaid were associated with sandstone (rather than siltstone) for the calculation of the subsidence curves.

In interpreting the shapes and the slopes of the subsidence curves, a critical aspect to take into account is the location of the well along a rift profile. The same geodynamic event generates different subsidence curves according to whether the data come from the rim basin, the rift shoulder, or a proximal or distal area of the main rift (Stampfli et al., 2001b). The Mermaid Nose is located in the proximal part of the rift branch, 60 km from the stable Pilbara Block (Figs. 1 and 2).

8. Discussion

During the Late Palaeozoic, the northeastern margin of Gondwana was affected by an extensional event associated with the opening of the Neotethys Ocean and the drifting of the Cimmerian terranes (Stampfli et al., 2001b). The northwestern Australian margin was also under the influence of this widespread event, coeval with the development of the so-called Westralian Superbasin (Yeates et al., 1987). This episode resulted in a thick and continuous infill additionally influenced by the impact of the Permo-Carboniferous Gondwanan glaciation (Bradshaw et al., 1994; Longley et al., 2002).

Fig. 9 shows drastic syn-rift tectonic subsidence during the Late Carboniferous–Early Permian (Asselian–Sakmarian). This initial phase is magnified by the development of the Mermaid Fault, responsible for the initial structure of the Mermaid Nose. The main activity along the fault is associated with the tilting of its footwall block (basement tilted block) and the development of a half-graben (Fig. 3). This episode predates the deposition of the Pennsylvanian?–Early Sakmarian glaciogenic Lyons Group (Fig. 3), and probably started during the Pennsylvanian.

This phase of extension, coeval with the development of the Westralian Superbasin, culminated in the separation of a continental sliver (Sibumasu on Fig. 10A) north of the Northern Carnarvon Basin during the Early Permian (Stampfli and Borel, 2002).

During the Permian, the Westralian Superbasin was separated from the incipient Neotethys ridge by the Argo-Burma and Gacu terranes (Fig. 10), and did not experience any seafloor spreading. This large depocentre therefore represents an aborted branch of the Neotethys rift system, which failed in favour of a trajectory between the Argo-Burma and Sibumasu terranes (Fig. 10).

This tectonic event also influenced the depositional setting of the Mermaid Nose. Based on the interpretation of the Lyons Group seismic facies (Figs. 3 and 4), a depositional model can be proposed with the newly formed half-graben probably acting as a glacial valley (Fig. 5). The inferred veneers of basal moraine (Figs. 3–5) reflect the presence of a shearing glacier or an ice tongue present within the Permo-Carboniferous half-graben. The periodic flooding of the half-graben during episodes of glacier melting and ice retreat could have generated the thicker paraglacial sections (Figs. 3–5). Therefore, the six stacked units (A1–B1 to A6–B6, Fig. 3) could be interpreted as six phases of advance/retreat of the glacier during Late Palaeozoic glaciation (Fig. 5).

Several elements suggest the presence of a terrestrial ice sheet that partially overlaid the western part of Australia during the Late Palaeozoic. Glacial striations have been identified on the bedrock overlain

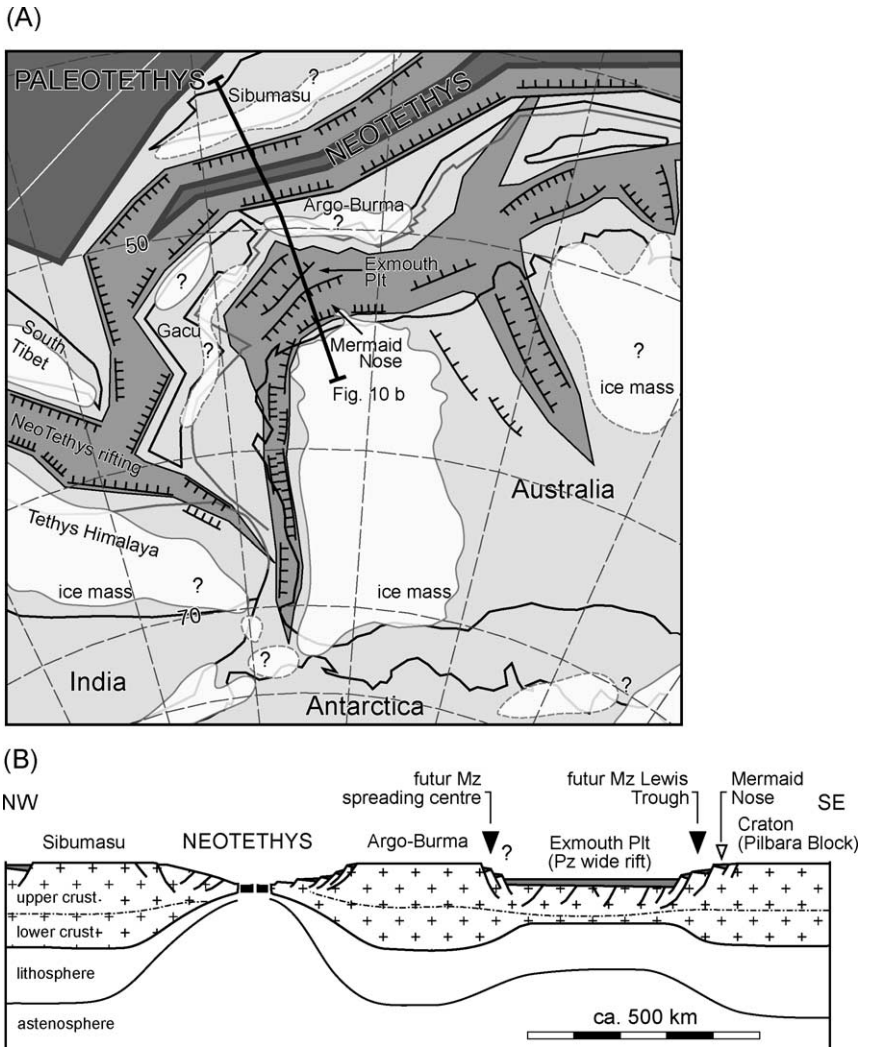

Fig. 10. (A) Regional reconstruction for the Sakmarian (modified from Borel and Stampfli, 2002) with the possible extension of the ice masses. (B) Generalised regional cross-section during the Sakmarian showing the structural elements and the terranes involved in the Palaeozoic and Mesozoic evolution of the north–western margin of Australia and the formation of the wide rift next to the Pilbara Block (no vertical scale).

by the Permo-Carboniferous Grant Group, on the southern margin (Yeates et al., 1984) and northern margin (Playford, 2002) of the Canning Basin. Redfern and Williams (2002) therefore suggest an ice sheet centred on the Pilbara Block, which probably expanded southward over the Yilgarn Craton (Eyles and de Broekert, 2001) (Fig. 10A). This hypothesis is supported by the presence of glacially eroded valleys on the eastern margin of the Pilbara Craton (Eyles and de Broekert, 2001), and the distribution of the Late Palaeozoic glaciogenic deposits located in depocentres along the Pilbara Block and the Yilgarn Craton, in the Perth Basin (Asselian Nangetty Formation), the Carnarvon Basin (Pennsylvanian?–Early Sakmarian Lyons Group), the Canning Basin (Asselian–Early Sakmarian Grant Group), and the Officer Basin (Asselian Paterson Formation). The presence of such an ice sheet is realistic, with an Australian northwestern margin lying at approximately 55°S during the Early Permian (Fig. 10, Baillie et al., 1994; Stampfli and Borel, 2002). The growth of glaciers could also have been locally

triggered by the development of relief associated with the Neotethys rift shoulder, as also proposed in Oman by Al-Belushi et al. (1996).

A worldwide eustatic sea-level rise occurred during the Sakmarian–Artinskian (Dickins, 1996; Wopfner, 1999), following the waning of Late Palaeozoic glaciation in Gondwana. In the Northern Carnarvon Basin, sedimentation changed from cold to warmer conditions (Archbold, 2002), and the deposition of carbonate and mud (Iasky et al., 2002) suggests post-glacial marine flooding.

The tectonic subsidence curves (Fig. 9) show the initial tectonic subsidence interrupted by an Early Permian "rebound", fading during the Permian. On the basis of the interpretation of the seismic facies, the post-glacial sequences forming a sedimentary wedge (Figs. 6 and 7) have been interpreted as an equivalent of the marine Callytharra Formation reported in several wells on the adjacent Peedamullah Shelf (Iasky et al., 2002). The first two Sakmarian–Artinskian seismic facies (sequences C and D1 on Figs. 6 and 7) display northwest-prograding patterns (Fig. 7A and B). Continuous extension or compaction of the underlying sediments can be inferred for the creation of accommodation space where these seaward-prograding sequences (sequences C and D1 on Figs. 6 and 7) were deposited during the early phase of post-glacial sedimentation. The top of the sedimentary wedge (sequences D2 and E on Fig. 7C and D) is characterised by landward-prograding patterns associated with a restricted truncation. An uplift event on the central part of the Mermaid Nose (Fig. 7C and D) could successfully explain both processes (i.e., landward progradation and truncations).

Based on the integration of the interpretation of the seismic data (Figs. 3, 5 and 7) with the subsidence curve (Fig. 9), it can be proposed that a Late Carboniferous onset of the rifting process, marked by the development of a half-graben, was followed by a (Late Pennsylvannian?) Asselian–Early Sakmarian syn-rift episode that was influenced by the impact of the Permo-Carboniferous glaciation. The end of the syn-rift phase, marked on the subsidence curve by a rebound (Fig. 9), coincides with the deposition of the Callytharra equivalent and a possible uplift of the Mermaid Nose.

Additionally, this event could reflect a ridge push episode characterising the onset of the Neotethys seafloor spreading, as already observed on the Neotethys margin (Stampfli et al., 2001b). Although no characteristic features of an intense inversion phase, such as compressive structures or strong evidence of an inverse displacement of the Mermaid Fault, have been unambiguously observed on the seismic data, such features could have been partially obliterated by the Jurassic–Cretaceous extensional event related to the rifting of the Argo Abyssal Plain.

The Wooramel and Byro Formations were deposited in the distal Dampier Sub-basin and the Northern Carnarvon Basin during the late Early Permian (Early–Middle Artinskian to Kungurian). On the Mermaid Nose, this period was characterised by a gap in sedimentation (Fig. 8), also observed on the Peedamullah Shelf (Iasky et al., 2002). Most of these fluvio-deltaic and shallow marine sediments probably bypassed the proximal part of the sub-basin. This non-deposition reflects a lack of accommodation space, possibly due to a delayed onset of the post-rift thermal subsidence (Fig. 9).

Following the deposition of the Kungurian–Tatarian Chinty Formation (Fig. 8), the Mermaid Nose is marked by a striking return of sedimentation with the thick (750 m on Fig. 8 and Table 1) Early Triassic Locker Formation. This deposit, mainly composed of shale, represents an original decompacted thickness of more than 1300 m, which translates into a subsidence rate greater than 150 m/Ma in order to accommodate the sequence. Therefore, in order to explain this subsidence rate illustrated by a pronounced break on the curves (Fig. 9), we suggest that a tectonic event, such as a reactivation of the Mermaid Fault, may have taken place in addition to the Early Triassic thermal subsidence.

During the late Early Jurassic to early Middle, a few restricted fault systems developed on the Mermaid Nose, probably associated with an early stage of the Argo Abyssal Plain rifting. This event is roughly coeval with the early development of the Lewis Trough (Fig. 2) that represents the main depocentres of the Dampier Sub-basin.

The most active tectonic phase related to the abyssal plains rifting occurred during the Late Jurassic, with the development of a southwest-trending graben that forms the main Mesozoic structure of the Mermaid Nose. Nevertheless, the subsidence curves (Fig. 9) do not display a well-marked step-

wise subsidence pattern that should theoretically characterise a margin affected by two successive phases of rifting. The second rifting phase, associated with the opening of the Argo Abyssal Plain, is illiustrated by a subtle break on the curve (thermal uplift?) followed by a renewal of subsidence during the Neocommian.

9. Conclusions

The tectonic subsidence curves calculated for the Mermaid Nose (Fig. 9) show a well marked event for the Permo-Carboniferous, with an initial pronounced tectonic subsidence followed by a rebound during the Early Permian.

Despite their relatively distant location from the Neotethys southern margin (Fig. 10A), the deposits of the Mermaid Nose still record the different phases of Late Palaeozoic rifting. The tectonic subsidence phase is associated with the development of a major normal fault and a half-graben, due to tilting of a basement block, which probably started during the Pennsylvanian. The filling of this depocentre was influenced, during the Pennsylvanian?–Early Sakmarian, by the impact of widespread continental glaciation, with the half-graben probably acting as a glacial valley. A late Sakmarian uplift event is observed on the subsidence curves (Fig. 9) and the seismic data (Figs. 6 and 7). This episode is possibly coeval with the onset of the Neotethys sea-floor spreading. Although similar Late Carboniferous–Early Permian rifting phases are well constrained on the eastern Gondwana margin, the onset of sea-floor spreading in these different locations (Lahul-Zanskar, Kasmir, Oman, Iran, Stampfli et al., 2001b) presents slightly younger ages than the possible interpreted ridge push episode on the Mermaid Nose (generally late? Early Permian to early Middle Permian in northwest India and in Oman (Batain area) to Middle Permian in the Oman mountains and in Sicily). This inferred diachronism of sea-floor spreading could emphasise the northwest progression of the Neotethys opening.

Admittedly, the Argo Abyssal Plain opening (and later the Gascoyn and Cuvier Abyssal Plains) affected the subsidence history of the Mermaid Nose (Kaiko and Tait, 2001 and Fig. 9), but this effect appears to be limited when compared to the impact of the Palaeozoic rifting. This Late Jurassic–Early Cretaceous event is coeval with the discrete uplift and the following subsidence observed on the curves (Fig. 9).

The subsidence modelling highlights the paradox of the Mermaid Nose by clearly emphasising the effects of the Late Carboniferous–Early Permian Neotethys rifting, whereas the extension coeval with the opening of the abyssal plains, which occurred later and closer to the Mermaid Nose, had only limited consequences. This result suggests a Late Palaeozoic, aborted rifting phase that affected a large part of the margin, including the craton shoulder, and which was followed by Late Jurassic–Early Cretaceous rifting, characterised by localised rifts whose impact was restricted to the central part of the Dampier Sub-basin (i.e., Lewis Trough, Fig. 2) and the western margin of the Exmouth Plateau (Fig. 1), where the sea-floor spreading took place during the drifting of the Gacu and Argo-Burma terranes (Fig. 10).

This concurs with the tectonic model of Gartrell (2000), which proposes two different extensional processes for the successive rifting phases. He suggests that the intermediate heat-flow conditions and crustal thickness during the Permo-Carboniferous imply a ductile behaviour of the lithosphere, resulting in a “wide rift” mode of extension mainly responsible for the development of the large Exmouth Plateau (Figs. 1, 2 and 10). This phase, which did not result in complete break-up and sea-floor spreading (Fig. 10B), also affected the studied area, located on the craton shoulder, with the tilting of a basement block and development of a half-graben (Fig. 3).

Then, during the Late Jurassic–Early Cretaceous rifting, when the margin was characterised by a thinned lithosphere more resistant to extension (Gartrell, 2000), the mode of extension changed to more narrow rifting, resulting in the development of localised extension processes (i.e., Lewis Trough and sea-floor spreading centre (Figs. 1, 2 and 10B)) at the eastern and western margins of the Permo-Carboniferous wide rift (i.e., Exmouth Plateau (Figs. 1, 2 and 10)). The geohistory of the Mermaid Nose (Fig. 9), although located less than 50 km of the Lewis Trough, does not illustrate a well-marked event for this episode, thus reflecting the limited effect of this extensional process on the thermal evolution of the area.

Acknowledgments

The authors wish to thank Apache Energy for access to seismic data and Schlumberger for the use of GeoFrame software. We thank M. Scheck-Wenderoth, R.A. Chadwick and C. Wijns for their review which helped to considerably improve the original manuscript. L.L. thanks the Swiss Academy of Sciences, the University of Lausanne, and the Société Académique Vaudoise for their financial support at the Tectonic Special Research Centre (TSRC) of the University of Western Australia (UWA). The TSRC and Myra Keep are also thanked for their support. G.D.B. thanks the Swiss National Foundation (SNF) for a post-doctoral grant at the Tectonic Special Research Centre of UWA. Project partly supported by SNF Grant number 2000-059188, 2000 20-100006/1. The subsidence curves have been calculated using a routine developed by J. Uriarte and R. Schegg of the University of Geneva and modified by G.D.B.

References

AGSO, N.W.S.S.G., 1994. Deep reflections on the North West shelf: changing perceptions of basin formation. In: Purcell, P.G., Purcell, R.R. (Eds.), The Sedimentary Basins of Western Australia: Proceedings of Petroleum Exploration Society of Australia Symposium. PESA, Perth, WA, pp. 63–76.

Al-Belushi, J.D., Glennie, K.W., Williams, B.P.J., 1996. Permo-Carboniferous glaciogenic Al Khlata Formation, Oman; a new hypothesis for origin of its glaciation. GeoArabia (Manama) 1 (3), 389–404.

Alsharhan, A.S., 1993. Late Palaeozoic glacial sediments of the southern Arabian Peninsula: their lithofacies and hydrocarbon potential. Marine and Petroleum Geology 10, 71–78.

Archbold, N.W., 2002. Peri-Gondwana permian correlations: the Meso-Tethyan margins. In: Keep, M., Moss, S.J. (Eds.), Proceedings of Petroleum Exploration Society of Australia Symposium, Perth, The Sedimentary Basins of Western Australia, vol. 3, pp. 223–240.

Baillie, P.W., Powell, C.M., Li, Z.X., Ryall, A.M., 1994. The tectonic framework of Western Australia's Neoproterozoic to recent sedimentary basins. In: Purcell, P.G., Purcell, R.R. (Eds.), The Sedimentary Basins of Western Australia: Proceedings of Petroleum Exploration Society of Australia Symposium. PESA, Perth, WA, pp. 45–62.

Baker, J.C., Havord, P.J., Martin, K.R., Ghori, K.A.R., 2000. Diagenesis and petrophysics of the early Permian Moogooloo Sandstone, southern Carnarvon Basin, Western Australia. AAPG Bulletin 84 (2), 250–265.

Barber, P., 1994. Sequence stratigraphy and petroleum potential of Upper Jurassic—Lower Cretaceous depositional systems in the Dampier Sub-Basin, North West Shelf, Australia. In: Purcell, P.G., Purcell, R.R. (Eds.), Proceedings of Petroleum Exploration Society of Australia Symposium, Perth, WA, The Sedimentary Basins of Western Australia, vol. 1, pp. 524–542.

Bond, G.C., Kominz, M.A., 1984. Construction of tectonic subsidence curves for the early Paleozoic miogeocline, southern Canadian Rocky Mountains: implications for subsidence mechanisms, age of break-up and crustal thinning. Geological Society of America Bulletin 95, 155–173.

Boote, D.R.D., Kirk, R.B., 1989. Depositional wedge cycles on evolving plate margin, Western and Northwestern. AAPG Bulletin 73 (2), 216–243.

Borel, G.D., Stampfli, G.M., 2002. Geohistory of the NW Shelf: a tool to assess the Phanerozoic motion of the Australian Plate. In: Keep, M., Moss, S.J. (Eds.), Proceedings of Petroleum Exploration Society of Australia Symposium, Perth, The Sedimentary Basins of Western Australia, vol. 3, pp. 119–128.

Boulton, G.S., 1978. Boulder shapes and grain-size distributions of debris as indicators of transport paths through a glacier and till genesis. Sedimentology 25 (6), 773–798.

Boulton, G.S., Deynoux, M., 1981. Sedimentation in glacial environments and the identification of tills and tillites in ancient sedimentary sequences. Precambrian Research 15 (3–4), 397–422.

Bradshaw, M.T., et al., 1994. Petroleum systems in West Australian Basins. In: Purcell, P.G., Purcell, R.R. (Eds.), The Sedimentary Basins of Western Australia: Proceedings of Petroleum Exploration Society of Australia Symposium. PESA, Perth, WA.

Crowley, A.J., Collins, E.S., 1996. The Stag oil field. APPEA Journal 36 (1), 130–141.

Dickins, J.M., 1996. Problems of a late Palaeozoic glaciation in Australia and subsequent climate in the Permian. In: Martini, I.P. (Ed.), Carboniferous–Permian Late Glacial and Postglacial Environments, Palaeogeography, Palaeoclimatology, Palaeoecology. Elsevier, Amsterdam, pp. 185–197.

Eyles, N., Young, G.M., 1994. Geodynamic controls on glaciation in Earth history. In: Deynoux, M., et al. (Ed.), Earth's Glacial Record. Cambridge University Press, pp. 1–22.

Eyles, N., de Broekert, P., 2001. Glacial tunnel valleys in the Eastern Goldfields of Western Australia cut below the late Paleozoic Pilbara ice sheet. Palaeogeography, Palaeoclimatology, Palaeoecology 171 (1–2), 29–40.

Eyles, N., Mullins, H.T., Hine, A.C., 1990. Thick and fast; sedimentation in a Pleistocene fiord lake of British Columbia, Canada. Geology (Boulder) 18 (11), 1153–1157.

Eyles, C.H., Mory, A.J., Eyles, N., 2003. Carboniferous–Permian facies and tectono-stratigraphic successions of the glacially influenced and rifted Carnarvon Basin, Western Australia. Sedimentary Geology 155 (1–2), 63–86.

Fullerton, L.G., Sager, W.W., Handschumacher, D.W., 1989. Late Jurassic to early Cretaceous evolution of the eastern Indian Ocean adjacent to north–west Australia. Journal of Geophysical Research 94 (3), 2937–2953.

Gartrell, A.P., 2000. Rheological controls on extensional styles and the structural evolution of the Northern Carnarvon Basin, North West Shelf, Australia. Australian Journal of Earth Sciences 47, 231–244.

Gorter, J.D., 1994. Triassic sequence stratigraphy of the Carnarvon Basin, Western Australia. In: Purcell, P.G., Purcell, R.R. (Eds.), Proceedings of Petroleum Exploration Society of Australia Symposium, Perth, WA, The Sedimentary Basins of Western Australia, vol. 2, pp. 397–413.

Gorter, J.D., Davies, J.M., 1999. Upper Permian carbonate reservoirs of the North West Shelf and Northern Perth Basin, Australia. APPEA Journal 39 (1), 343–362.

Hill, G., 1994. The role of pre-rift structure in the architecture of the Dampier Basin area, North West Shelf, Australia. APEA Journal 34 (1), 602–613.

Hocking, R.M., 1990. Carnarvon Basin, Geology and mineralogy resources of Western Australia. Western Australia Geological Survey, 457–495.

Hocking, R.M., Moors, H.T., Van de Graaff, J.E., 1987. Geology of the Carnarvon Basin, Western Australia. Bulletin of the Geological Survey of Western, 133.

Hocking, R.M., Mory, A.J., Williams, I.R., 1994. An atlas of Neoproterozoic and Phanerozoic basins of Western Australia. In: Purcell, P.G., Purcell, R.R. (Eds.), The Sedimentary Basins of Western Australia: Proceedings of Petroleum Exploration Society of Australia Symposium. PESA, Perth, WA, pp. 21–43.

Iasky, R.P., Mory, A.J., Blundell, K.A., Ghori, K.A.R., 2002. Prospectivity of the Peedamullah Shelf and Onslow Terrace revisited. In: Keep, M., Moss, S.J. (Eds.), Proceedings of Petroleum Exploration Society of Australia Symposium, Perth, The Sedimentary Basins of Western Australia, vol. 3.

Jablonski, D., 1997. Recent advances in the sequence stratigraphy of the Triassic to lower Cretaceous succession in the Northern Carnarvon Basin, Australia. APPEA Journal 36 (1), 429–454.

Kaiko, A.R., Tait, A.M., 2001. Post-rift tectonic subsidence and palaeo-water depths in the Northern Carnarvon Basin, Western Australia. APPEA Journal 41 (1), 367–379.

Labutis, V.R., 1994. Sequence stratigraphy and the NorthWest Shelf of Australia. In: Purcell, P.G., Purcell, R.R. (Eds.), Proceedings of Petroleum Exploration Society of Australia Symposium, Perth, WA, The Sedimentary Basins of Western Australia, vol. 2, pp. 159–180.

Levell, B.K., Braakman, J.H., Rutten, K.W., 1988. Oil-bearing sediments of the Gondwana glaciation in Oman. AAPG Bulletin 72, 775–796.

Longley, I.M., et al., 2002. The North West Shelf of Australia—a Woodside perspective. In: Keep, M., Moss, S.J. (Eds.), Proceedings of Petroleum Exploration Society of Australia Symposium, Perth, WA, The Sedimentary Basins of Western Australia, vol. 3, pp. 27–88.

Miller, L.R., Smith, S.A., 1996. The development and regional significance of rift-related depositional systems in the Dampier sub-basin. APPEA Journal 36 (1), 369–384.

Mishra, H.K., 1996. Comparative petrological analysis between the Permian coals of India and Western Australia; paleoenvironments and thermal history. In: Martini, I.P. (Ed.), Carboniferous-Permian Late Glacial and Postglacial Environments, Palaeogeography, Palaeoclimatology, Palaeoecology. Elsevier, Amsterdam, pp. 199–216.

Mitchum, R.M., Vail, P.R., Sangree, J.B., 1977. Seismic stratigraphy and global changes of sea level: Part 6. Seismic interpretation of seismic reflection patterns in depositional sequences. In: Payton, C.E. (Ed.), Seismic Stratigraphy—Aplications to Hydrocarbon Exploration. AAPG, Tulsa, pp. 117–133.

Mory, A.J., Backhouse, J., 1997. Permian stratigraphy and palynology of the Carnarvon Basin, Western Australia. Geological Survey of Western Australia, vol. 46. (Perth).

Pfiffner, O.A., et al., 1997. Incision and backfilling of Alpine valleys: Pliocene, Pleistocene and Holocene processes. In: Pfiffner, O.A., Lehner, P., Heitzman, P.Z., Mueller, S., Steck, A. (Eds.), Deep Structure of the Swiss Alps—Results from NRP 20. Birkhäuser, Basel, pp. 265–288.

Playford, P., 2002. Palaeokarst, pseudokarst, and sequence stratigraphy in Devonian reef complexes of the Canning Basin, Western Australia. In: Keep, M., Moss, S.J. (Eds.), Proceedings of Petroleum Exploration Society of Australia Symposium, Perth, The Sedimentary Basins of Western Australia, vol. 3, pp. 763–793.

Potter, P.E., Franca, A.B., Spencer, C.W., Caputo, M.V., 1995. Petroleum in glacially related sandstones of Gondwana: a review. Journal of Petroleum Geology 18 (4), 397–420.

Pryer, L.L., Romine, K.K., Loutit, T.S., Barnes, R.G., 2002. Carnarvon basin architecture and structure defined by the integration of mineral and petroleum exploration tools and techniques. APPEA Journal, 287–309.

Redfern, J., Williams, B.P.J., 2002. Canning Basin Grant Group glaciogenic sediments: part of the Gondwanan Permo-Carboniferous hydrocarbon province. In: Keep, M., Moss, S.J. (Eds.), Proceedings of Petroleum Exploration Society of Australia Symposium, Perth, The Sedimentary Basins of Western Australia, vol. 3, pp. 851–871.

Romine, K.K., Durrant, J.M., Cathro, D.L., Bernardel, G., 1997. Petroleum play element prediction for the Cretaceous–Tertiary basin phase, Northern Carnarvon Basin. APPEA Journal 37 (1), 315–338.

Sclater, J.G., Christie, P.A.F., 1980. Continental stretching: an explanation of the post-mid-Cretaceous subsidence of the central North Sea basin. Journal of Geophysical Research 85 (B7), 3711–3739.

Stagg, H.M.J., Colwell, J.B., 1994. The structural foundations of the Northern Carnarvon basin. In: Purcell, P.G., Purcell, R.R. (Eds.), Proceedings of Petroleum Exploration Society of Australia Symposium, Perth, WA, The Sedimentary Basins of Western Australia, pp. 349–364.

Stampfli, G.M., 2000. Tethyan oceans. In: Bozkurt, E., Winchester, J.A., Piper, J.D.A. (Eds.), Tectonics and Magmatism in Turkey and the Surroundings Area, Geological Society of London, Special Publication, London, pp. 1–23.

Stampfli, G.M., Borel, G.D., 2002. A Plate Tectonic Model for the Paleozoic and Mesozoic constrained by dynamic plate boundaries and restored synthetic oceanic isochrons. Earth and Planetary Science Letters 196 (1–2), 17–33.

Stampfli, G.M., Borel, G.D., Cavazza, W., Mosar, J., Ziegler, P.A. (Eds.), 2001a. The Paleotectonic Atlas of the PeriTethyan Domain. European Geophysical Society.

Stampfli, G.M., Mosar, J., Favre, P., Pillevuit, A., Vannay, J.-C., 2001b. Permo-Mesozoic Evolution of the Western Tethyan Realm: The Neotethys/East- Mediterranean Basin Connection. In: Cavazza, W., Robertson, A.H.F.R., Ziegler, P.A., Crasquin-Soleau, S. (Eds.), Peritethyan Rift/Wrench Basins and Passive Margins, IGCP vol. 369. Museum Natn. Hist. Nat, Paris, pp. 51–108.

Veevers, J.J., 2000. Australia's Neigbours in Gondwanaland along the Tethyan margin. In: Veevers, J.J. (Ed.), Billion-Year Earth History of Australia and Neighbours in Gondwanaland. GEMOC, Sydney, pp. 309–324.

Westphal, H., Aigner, T., 1997. Seismic stratigraphy and subsidence analysis in the Barrow-Dampier subbasin, Northwest Australia. AAPG Bulletin 81 (10), 1721–1749.

Wopfner, H., 1999. The Early Permian deglaciation event between East Africa and northwestern Australia. In: Storey, B.C., Rubridge, B.S., Cole, D.I., De, W.M.J. (Eds.), Gondwana-10; Event Stratigraphy of Gondwana; Proceedings, Journal of African Earth Sciences, vol. 1. Pergamon, London, pp. 77–90. International.

Yasin, A.R., Iasky, R.P., 1998. Petroleum geology of the Peedamullah Shelf, Northern Carnarvon Basin. In: Purcell, P.G., Purcell, R.R. (Eds.), Proceedings of Petroleum Exploration Society of Australia Symposium, Perth, WA, The Sedimentary Basins of Western Australia, vol. 2, pp. 473–490.

Yeates, A.N., Gibson, D.L., Towner, R.R., Crowe, E.W.A., 1984. Regional geology of the onshore Canning Basin, Western Australia. In: Purcell, P.G. (Ed.), The Canning Basin, Western Australia: Proceedings of the Petroleum Exploration Society of Australia. PESA, Perth, pp. 23–56.

Yeates, A.N., et al., 1987. The Westralian Superbasin: an Australian link with Tethys. In: McKenzie, K.G. (Ed.), Shallow Tethys, vol. 2. A. A. Balkema, Rotterdam, Netherlands, pp. 199–213.

Young, H.C., Lemon, N.M., Hull, J.N.F., 2001. The Middle Cretaceous to Recent sequence stratigraphic evolution of the Exmouth-Barrow margin, Western Australia. APPEA Journal 41 (1), 381–413.